GHGT-9

Influence of viscosity and surface tension on the effective mass transfer area of structured packing

Robert E. Tsai[a], A. Frank Seibert[a], R. Bruce Eldridge[a], and Gary T. Rochelle[a,*]

[a]Department of Chemical Engineering, The Separations Research Program, The University of Texas at Austin, Austin, Texas 78712, USA

Abstract

The effective mass transfer area (a_e) of three structured packings (Mellapak 250Y, Mellapak 500Y, and Flexipac 1Y) was measured via chemical absorption in a 0.427 m ID column as a function of liquid load (1-30 gpm/ft^2 or 2.4-73.2 m^3/m^2·h), liquid viscosity (1-15 mPa·s), and surface tension (30-72 mN/m). Viscosity had no effect and surface tension had only a weak effect on the effective area. The ratio of effective area to specific surface area (a_e/a_p) was correlated as a function of the liquid Weber and Froude numbers within limits of ±15% for the entire experimental database:

$$\frac{a_e}{a_p} = 1.362\left[(We_L)(Fr_L)^{-\frac{1}{3}}\right]^{0.122}$$

Keywords: CO$_2$ absorption; structured packing; packed column; effective area; viscosity; surface tension

1. Introduction

Packed columns are commonly used in absorption and stripping processes to provide efficient gas-liquid contacting. A reliable model for the effective mass transfer area (a_e) of the packing is important for design and analysis of these systems. It is especially critical for CO$_2$ capture by amine absorption, because the CO$_2$ absorption rate typically becomes independent of conventional mass transfer coefficients (k_G or k_L^0) but remains directly proportional to the effective area.

Wang et al. [1] provided a comprehensive review of the numerous packing area correlations in the literature. None have been shown to be truly predictive over a wide range of conditions. Different and sometimes even contradictory effects of viscosity and surface tension on the effective area are predicted. The various amine solvents that are being considered for CO$_2$ capture have a range of viscosities and surface tensions [2-4], and therefore, a dependable model is needed to predict these effects.

The influence of liquid viscosity and surface tension on the effective mass transfer area of structured packing was determined by absorption of CO$_2$ into dilute caustic solution. With excess free hydroxide, the concentration of bicarbonate (HCO$_3^-$) is negligible, and the overall reaction may be written as:

$$CO_2(aq) + 2OH^- \rightarrow CO_3^{2-} + H_2O \tag{1}$$

---

* Corresponding author. Tel.: +1-512-471-7230; fax: +1-512-471-7824.
E-mail address: gtr@che.utexas.edu.

The reaction can be considered as practically irreversible, with a rate expression given by equation 2.

$$r = k_{OH^-}[OH^-][CO_2]$$ (2)

When CO_2 partial pressures are low and hydroxide ion is present in relative excess, the reaction can be treated as pseudo-first-order. Equation 2 consequently simplifies to:

$$r \cong k_1[CO_2]$$ (3)

2. Experimental

2.1 Packed column

The packed column had an outside diameter of 0.46 m, an inside diameter of 0.427 m, and a 3-m packed height. Operation was countercurrent, with ambient air entering below the packing bed and flowing upward through the tower. The liquid (typically 0.75 m^3 inventory) was pumped in a closed loop and was distributed at the top of the column using a pressurized fractal distributor with 108 drip points/m^2. See Tsai et al. [5] for more details.

2.2 Wetted-wall column (WWC)

The wetted-wall column (WWC) was a bench-scale gas-liquid contactor with a known interfacial area (38.52 cm^2) that was used to measure the kinetics of various systems. The apparatus has previously been used and described by Bishnoi and Rochelle [6], Cullinane and Rochelle [7], and Tsai et al. [5].

2.3 Supplementary equipment

The goniometer (ramé-hart Inc., model #100-00) included an adjustable stage, a syringe support arm, a computer-linked camera for live image display, and a light source. This system was used with FTA32 Video 2.0 software (developed by First Ten Angstroms, Inc.) to make surface tension measurements via pendant drop analysis.

A Physica MCR 300 rheometer (Anton Paar, USA) equipped with a cone-plate spindle (CP 50-1) was used for viscosity measurements. Temperature was regulated (± 0.1°C) with a Peltier unit (TEK 150P-C) and a Julabo F25 water bath unit (for counter-cooling). Measurement profiles typically consisted of a logarithmically ramped shear rate (100-500 s^{-1}), with a minimum of 10 points taken at 15 second intervals.

2.4 Chemical reagents

A nonionic surfactant, Tergitol NP-7 (Dow), was used to reduce the surface tension of solutions. POLYOX WSR N750 (Dow) – essentially, poly(ethylene oxide) with a molecular weight of 300,000 – was employed as a viscosity enhancer. With both of these reagents, suppression of foam was found to be necessary, particularly during packed column experiments. Dow Corning Q2-3183A antifoam was utilized for this purpose.

3. Results and Discussion

3.1 Theoretical analysis of data

The performance of both the WWC and the packed column was modeled by series resistance (equation 4). The overall mass transfer resistance is the sum of the gas- and liquid-side resistances.

$$\frac{1}{K_G} = \frac{1}{k_G} + \frac{1}{k_g'}$$ (4)

For the WWC, the overall mass transfer coefficient (K_G) was determined from the CO_2 flux and the partial pressure driving force. The gas-side mass transfer coefficient (k_G) was a function of physical properties and was calculated using a correlation that was developed by absorption of SO_2 into NaOH solution, an entirely gas-film controlled process [6]. K_G and k_G were used to calculate k_g', which has been defined as a liquid-side mass transfer coefficient expressed in terms of a CO_2 partial pressure driving force.

$$N_{CO_2} = k_g{}' \left(P_{CO_2}^i - P_{CO_2}^* \right) = k_g{}' P_{CO_2}^i \tag{5}$$

In equation 5, P_{CO2}^* is zero because of the irreversibility of the CO_2-NaOH reaction. Under the assumption of pseudo-first-order conditions, surface renewal theory may be used to present the flux as [8]:

$$N_{CO_2} = k_L^0 \sqrt{1 + \frac{k_1 D_{CO_2,L}}{\left(k_L^0\right)^2}} \frac{P_{CO_2}^i}{H_{CO_2}} = k_L^0 \sqrt{1 + Ha^2} \frac{P_{CO_2}^i}{H_{CO_2}} \tag{6}$$

Ha^2 was on the order of 10^2 in the WWC, so equation 6 was simplified to:

$$N_{CO_2} = \frac{\sqrt{k_1 D_{CO_2,L}}}{H_{CO_2}} P_{CO_2}^i \tag{7}$$

Thus, from equations 5 and 7, we have the following theoretical expression for k_g'.

$$k_g{}' = \frac{\sqrt{k_1 D_{CO_2,L}}}{H_{CO_2}} = \frac{\sqrt{k_{OH^-}[OH^-]D_{CO_2,L}}}{H_{CO_2}} \tag{8}$$

Measured k_g' values were compared with calculated ones, evaluated using literature values for the terms in equation 8. The correlations for the diffusion coefficient ($D_{CO2,L}$), Henry's constant (H_{CO2}), and reaction rate constant (k_{OH^-}) were based on the work of Pohorecki and Moniuk [9].

For the packed column experiment, gas-side resistance was intentionally limited by using dilute caustic solution (0.1 kmol/m³) and operating at high superficial air velocities (0.6, 1.0, or 1.5 m/s). This resistance was estimated to account for 1% of the overall mass transfer resistance, with k_G calculated from the correlation of Rocha et al. [10]. The $1/k_G$ term in equation 4 was ignored, and K_G was assumed to be equal to k_g'. This approximation enabled the effective area (a_e) to be determined by separating it from the volumetric mass transfer coefficient, $K_G a_e$.

$$a_e = \frac{u_G \ln\left(\frac{y_{CO_2,in}}{y_{CO_2,out}}\right)}{Z K_G RT} \approx \frac{u_G \ln\left(\frac{y_{CO_2,in}}{y_{CO_2,out}}\right)}{Z k_g{}' RT} = \frac{u_G \ln\left(\frac{y_{CO_2,in}}{y_{CO_2,out}}\right)}{Z RT} \cdot \frac{H_{CO_2}}{\sqrt{k_{OH^-}[OH^-]D_{CO_2,L}}} \tag{9}$$

k_g' was calculated with equation 8, although the $Ha^2 \gg 1$ approximation was weaker in these experiments. Ha^2 was around 15 in the worst case scenario, with k_L^0 estimated from the correlation of Rocha et al. [10].

3.2 Results with the wetted-wall column (WWC)

The WWC had two purposes. First, it was used to validate the baseline CO_2-NaOH kinetics – that is, k_g' calculated using the equations of Pohorecki and Moniuk [9]. Second, it was employed to test for potential impacts of the property-modifying additives (Tergitol NP-7 or POLYOX WSR N750) on k_g'. The WWC results are summarized in Table 1, expressed as a normalized k_g' (experimental k_g' / calculated k_g').

Table 1. Summary of WWC results

Test system	Approx. μ_L and/or σ	Number of data points	Normalized k_g'
0.1 kmol/m³ NaOH	0.75 mPa·s, 72 mN/m	111	1.10 ± 0.09
0.1 kmol/m³ NaOH + 125 ppm$_v$ Tergitol NP-7 + 50 ppm$_{w/v}$ Dow Corning Q2-3183A antifoam	30 mN/m	32	1.08 ± 0.07
0.1 kmol/m³ NaOH + 1.25 wt % POLYOX WSR N750	7.5 mPa·s	10	0.91 ± 0.05

The baseline measurements gave values of flux (k_g') that were 10% higher than predicted by the parameters from Pohorecki and Moniuk [9]. Nevertheless, the disparity was not believed to be drastic enough to reject the use of their correlations. The "Pohorecki" k_g' was therefore assumed to be applicable in the interpretation of the packed column results. There was no statistically confirmable impact of surfactant and antifoam, implying that the same k_g' could be applied for this system as well.

Possible explanations for this result are discussed in Tsai et al. [5]. The effect of POLYOX WSR N750 was rather interesting. Given the fairly low concentration of polymer, one would not anticipate any major effects on k_{OH^-} or H_{CO2} [11]. A ten-fold viscosity increase would, however, be expected to cause an equivalent decrease in the diffusion coefficient, which consequently would reduce k_g' by a factor of 3. This was clearly not the case, as the data exhibited only a minor depression in k_g' relative to the baseline. A survey of the literature revealed that this result was, in fact, quite justifiable. Several different studies have confirmed a unique feature of dilute, aqueous polymer solutions: limited influence on the diffusivity of small molecules like CO_2. Komiyama and Fuoss [12] postulated that while the bulk viscosity of a solution might be enhanced by entanglement of long polymer chains, considerable freedom should still exist for the localized movement of chain segments and of small molecules around these segments. In other words, the local viscosity should be significantly lower than the bulk viscosity, and thus, the CO_2 diffusion rates in polymer solutions and in pure solutions should not differ too much. Lohse et al. [13] measured CO_2 diffusion in aqueous polymer solutions and correlated their results in the form of equation 10. The subscripts 0 and P respectively refer to pure solution and polymer.

$$\frac{D_{CO_2,L}}{D_{CO_2,0}} = \left(\frac{\mu_L}{\mu_0}\right)^{-3.7\sqrt{\frac{M_0}{M_P}}} \tag{10}$$

The WWC data displayed a somewhat larger reduction in k_g' than that predicted by equation 10, but they were still in far better agreement with the "polymer" theory than with the "standard" theory (inverse 1:1 relationship of diffusivity-viscosity). Equation 10 was concluded to be valid, and for the packed column experiments conducted with POLYOX WSR N750, the diffusion coefficient in equation 8 was modified accordingly.

The WWC tests with POLYOX did not include antifoam (Table 1). Additional experiments will be performed that incorporate this additive; however, for the moment, its presence has been assumed to have no influence on k_g'.

3.3 Mass transfer area measurements

One of the packings characterized in this work was Sulzer Mellapak 250Y, a standard high capacity structured packing (a_p = 250 m^2/m^3). The data could not be differentiated with respect to air velocity (0.6, 1.0, or 1.5 m/s) and are plotted in Figure 1.
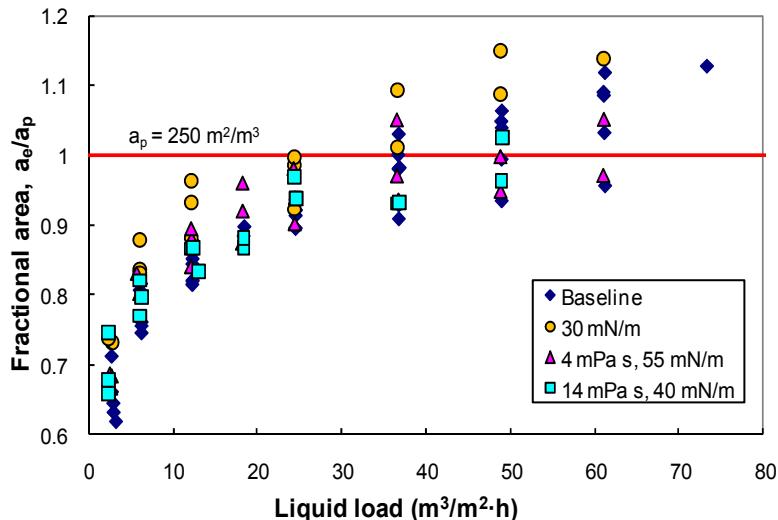

Figure 1. Fractional area data for Mellapak 250Y.

Tests with Tergitol NP-7 or POLYOX WSR N750 required antifoam, which was generally used in quantities no greater than 100 ppm$_{w/v}$. It was not possible to increase viscosity without also affecting surface tension because of the POLYOX WSR N750 itself, as well as the antifoam; hence the reduced surface tensions of the viscous systems. The fractional areas for Mellapak 250Y were quite high, indicating the surface area was being well utilized. Lowering the surface tension to 30 mN/m appeared to result in a marginal increase in the measured area, but this could not be definitively concluded, given the inherent experimental error

(~10%). Viscosity had no impact on the effective area. Thus, it would seem that the mass transfer area of Mellapak 250Y is relatively insensitive to physical property variations. This is in contrast to a high surface area packing such as Mellapak 500Y, where surface tension appears to play a significant role, likely because of the greater prominence of capillary phenomena (i.e. liquid pooling and bridging) [5,14].

3.4 Global model

The current experimental database consists of three different structured packings (Mellapak 250Y, Mellapak 500Y, and Flexipac 1Y), tested over a range of liquid viscosities (1-15 mPa·s) and surface tensions (30-72 mN/m). Table 2 lists the relevant physical dimensions of the packings, which were defined in the same manner as in the work of Sidi-Boumedine and Raynal [15].

Table 2. Packing parameters

Packing	Specific area, a_p (m^2/m^3)	Channel side, S (mm)	Channel base, B (mm)	Crimp height, h (mm)
Sulzer Mellapak 250Y (M250Y)	250	17	24.1	11.9
Sulzer Mellapak 500Y (M500Y)	500	8.1	9.6	6.53
Koch-Glitsch Flexipac 1Y (F1Y)	410	9	12.7	6.4

An attempt was made to correlate the entire database in the form of dimensionless groups. It has been our experience that below the flooding limit, gas properties (e.g. superficial velocity) have no impact on the effective area of structured packing. The modeling effort was therefore based solely on liquid parameters. The characteristic length, δ, was defined as the thickness of the liquid film on the packing surface. Likewise, the liquid velocity, u_L, was a calculated average film velocity. The "classical" equations for film flow on an inclined flat plate, as presented by Bird et al. [16] (among others), were assumed to apply. The film thickness equation is expressed below.

$$\delta = \sqrt{\frac{3 u_L \mu_L}{\rho_L g \sin\alpha}} = \sqrt[3]{\frac{3\mu_L}{\rho_L g \sin\alpha} \frac{Q}{L_p}} \qquad (11)$$

The wetted perimeter (L_p) was calculated by equation 12.

$$L_p = \frac{4S}{Bh} A \qquad (12)$$

It was found that the data aligned quite well when plotted as a function of $(We_L)(Fr_L)^{-1/3}$, as shown in Figure 2. Practically all of the points fall within 15% of the regressed correlation (equation 13).

$$\frac{a_e}{a_p} = 1.362\left[(We_L)(Fr_L)^{-1/3}\right]^{0.122} = 1.362\left[\frac{\rho_L}{\sigma} g^{1/3}\left(\frac{Q}{L_p}\right)^{4/3}\right]^{0.122} \qquad (13)$$

An expansion of $(We_L)(Fr_L)^{-1/3}$ to individual physical parameters reveals that the effective area is predicted to be most strongly tied to the liquid flow rate and packing geometry. Liquid density and surface tension are significant as well, although the correlation fails to capture the distinct surface tension/geometry relation that has been observed [5]. Viscosity is notably absent from equation 13, which is consistent with our current findings. There is also no predicted effect of corrugation angle, which has been held constant (45°) in the tests performed thus far.
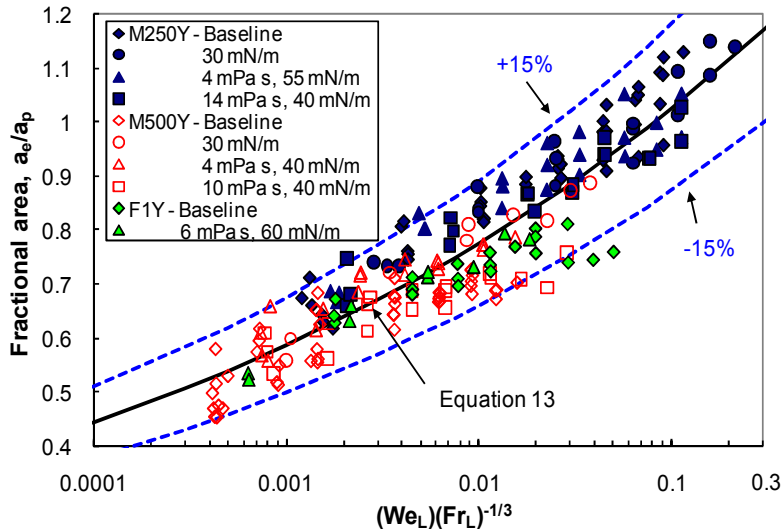
Figure 2. Structured packing mass transfer area database, compared
with global correlation (equation 13).

The Separations Research Program (SRP) at the University of Texas has compiled a large database of effective area measurements. Figure 3 presents results obtained with a non-perforated 250-series structured packing using a gravity-fed orifice pipe liquid distributor with 430 drip points/m^2. The data are compared with the predictions from equation 13 and two widely used models: Rocha-Bravo-Fair [10] and Billet-Schultes [17]. Equation 13 matches the data well, especially at the higher liquid loads. One would expect the packing surface to be well wetted at high liquid loads, on account of the relatively open geometry. However, even near 80 m^3/m^2·h, both Rocha-Bravo-Fair and Billet-Schultes predict fractional areas far from unity. It is worth noting that the literature models were primarily inferred from distillation data, generally consisting of systems with very low surface tensions. Furthermore, validation was strictly with overall mass transfer results (e.g. $K_G a_e$); a_e itself was not independently verified. Caution should be exercised when modeling the effective area of structured packing with these correlations at high surface tensions.
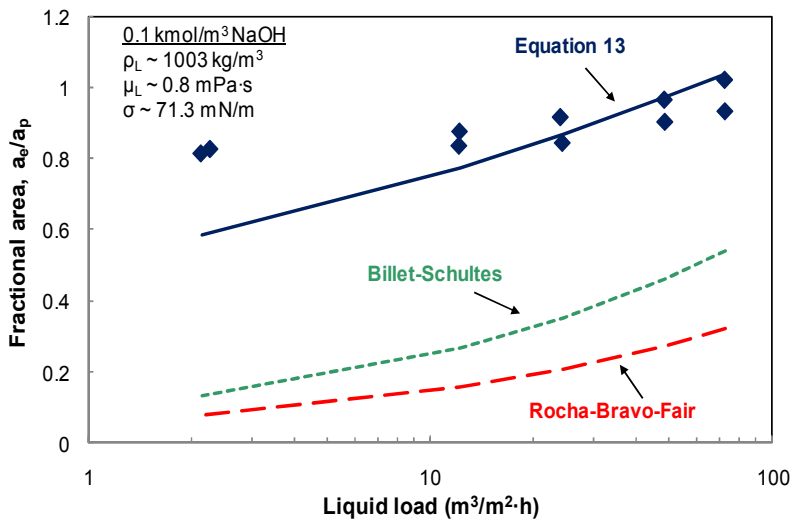

Figure 3. Comparison of prototype 250-series packing data (points) with
models. a_p = 250 m^2/m^3; L_p = 35.272 m.

4. Conclusions

Rates of absorption of CO_2 into 0.1 kmol/m³ NaOH were measured. The value of k_g' was found to be 10% greater than predicted by the correlation of Pohorecki and Moniuk [9]. Use of their correlation was nevertheless believed to be acceptable. The addition of Tergitol NP-7 surfactant (125 ppm$_v$) and Dow Corning Q2-3183A antifoam (50 ppm$_{w/v}$) did not appreciably affect k_g'. The presence of POLYOX WSR N750 (1.25 wt %) only resulted in a small depression in k_g', which was actually in close agreement with the theory discussed in the literature.

The effective mass transfer areas of three structured packings (Mellapak 250Y, Mellapak 500Y, and Flexipac 1Y) were measured via absorption of CO_2 into caustic solution. No dependence on liquid viscosity (1-15 mPa·s) was observed. Surface tension was found to be important for M500Y but not for M250Y; the interfacial area of M500Y increased significantly when surface tension was lowered to 30 mN/m. The mass transfer area database was represented well (±15%) by the correlation that was regressed as a function of $(We_L)(Fr_L)^{-1/3}$.

5. Acknowledgment

6. Nomenclature

A = cross-sectional area of packed column, m²
a_e = effective area of packing, m²/m³
a_p = specific surface area of packing, m²/m³
B = packing channel base, m
D_{CO2} = diffusivity of CO_2, m²/s
g = gravitational constant, m/s²
H_{CO2} = Henry's constant of CO_2, m³·Pa/kmol
h = packing crimp height, m
K_G = overall gas-side mass transfer coefficient, kmol/m²·Pa·s
k_1 = pseudo-first-order reaction rate constant, s⁻¹
k_G = gas-side mass transfer coefficient, kmol/m²·Pa·s
k_g' = liquid-side mass transfer coefficient, kmol/m²·Pa·s
k_L^0 = physical liquid-side mass transfer coefficient, m/s
k_{OH-} = second-order reaction rate constant, m³/kmol·s
L_p = wetted perimeter in cross-sectional slice of packing, m
M = molecular weight, kg/kmol
N_{CO2} = molar flux of CO_2, kmol/m²·s
P^*_{CO2} = equilibrium partial pressure of CO_2, Pa
P^i_{CO2} = partial pressure of CO_2 at gas-liquid interface, Pa
Q = volumetric flow rate, m³/s
R = ideal gas constant, m³·Pa/kmol·K
r = chemical reaction rate, kmol/m³·s
S = packing channel side, m
T = absolute temperature, K
u = velocity, m/s
$y_{CO2,in/out}$ = mole fraction of CO_2 at inlet/outlet
Z = packed height, m

Greek Symbols

α = corrugation angle (with respect to the horizontal), deg
δ = film thickness, m
μ = viscosity, Pa·s
ρ = density, kg/m³
σ = surface tension, N/m

Subscripts

G = gas phase
L = liquid phase

Dimensionless Groups

a_f = fractional area of packing, a_e/a_p
Fr = Froude number, $u^2/g{\cdot}\delta$
Ha = Hatta number, $(k_1 D_{CO2,L})^{0.5}/k_L^0$
We = Weber number, $\rho u^2 \delta/\sigma$

7. References

1. G.Q. Wang, X.G. Yuan, and K.T. Yu, Review of Mass-Transfer Correlations for Packed Columns, *Ind. Eng. Chem. Res.* 44 (2005) 8715.
2. R.H. Weiland, J.C. Dingman, D.B. Cronin, and G.J. Browning, Density and Viscosity of Some Partially Carbonated Aqueous Alkanolamine Solutions and Their Blends, *J. Chem. Eng. Data* 43 (1998) 378.
3. G. Vázquez, E. Alvarez, J.M. Navaza, R. Rendo, and E. Romero, Surface Tension of Binary Mixtures of Water + Monoethanolamine and Water + 2-Amino-2-methyl-1-propanol and Tertiary Mixtures of These Amines with Water from 25°C to 50°C, *J. Chem. Eng. Data* 42 (1997) 57.
4. A. Henni, J.J. Hromek, P. Tontiwachwuthikul, and A. Chakma, Volumetric Properties and Viscosities for Aqueous AMP Solutions from 25°C to 70°C, *J. Chem. Eng. Data* 48 (2003) 551.
5. R.E. Tsai, P. Schultheiss, A. Kettner, J.C. Lewis, A.F. Seibert, R.B. Eldridge, and G.T. Rochelle, Influence of Surface Tension on Effective Packing Area, *Ind. Eng. Chem. Res.* 47 (2008) 1253.
6. S. Bishnoi and G.T. Rochelle, Absorption of Carbon Dioxide into Aqueous Piperazine: Reaction Kinetics, Mass Transfer and Solubility, *Chem. Eng. Sci.* 55 (2000) 5531.
7. J.T. Cullinane and G.T. Rochelle, Kinetics of Carbon Dioxide Absorption into Aqueous Potassium Carbonate and Piperazine, *Ind. Eng. Chem. Res.* 45 (2006) 2531.
8. P.V. Danckwerts, *Gas-Liquid Reactions*, McGraw-Hill Book Company, New York, 1970.
9. R. Pohorecki and W. Moniuk, Kinetics of Reaction between Carbon Dioxide and Hydroxyl Ions in Aqueous Electrolyte Solutions, *Chem. Eng. Sci.* 43 (1988) 1677.
10. J.A. Rocha, J.L. Bravo, and J.R. Fair, Distillation Columns Containing Structured Packings: A Comprehensive Model for Their Performance. 2. Mass-Transfer Model, *Ind. Eng. Chem. Res.* 35 (1996) 1660.
11. E. Rischbieter, A. Schumpe, and V. Wunder, Gas Solubilities in Aqueous Solutions of Organic Substances, *J. Chem. Eng. Data* 41 (1996) 809.
12. J. Komiyama and R.M. Fuoss, Conductance in Water-Poly(vinyl alcohol) Mixtures, *Proc. Natl. Acad. Sci. U.S.A.* 69 (1972) 829.
13. M. Lohse, E. Alper, G. Quicker, and W.D. Deckwer, Diffusivity and Solubility of Carbon Dioxide in Diluted Polymer Solutions, *AIChE J.* 27 (1981) 626.
14. C.W. Green, J. Farone, J.K. Briley, R.B. Eldridge, R.A. Ketcham, and B. Nightingale, Novel Application of X-ray Computed Tomography: Determination of Gas/Liquid Contact Area and Liquid Holdup in Structured Packing, *Ind. Eng. Chem. Res.* 46 (2007) 5734.
15. R. Sidi-Boumedine and L. Raynal, Influence of the Viscosity on the Liquid Hold-up in Trickle-bed Reactors with Structured Packings, *Catal. Today* 105 (2005) 673.
16. R.B. Bird, W.E. Stewart, and E.N. Lightfoot, *Transport Phenomena* (2nd ed.), John Wiley & Sons, Inc., New York, 2002.
17. R. Billet and M. Schultes, Predicting Mass Transfer in Packed Columns, *Chem. Eng. Technol.* 16 (1993) 1.